Thermal Inspection of Low Emissivity Surfaces Using a Pulsed Light Emitting Diodes (PLED) Heat Source

Joseph N. Zalameda*, Peter W. Spaeth, and Samuel J. A. Hocker

NASA Langley Research Center Hampton, VA 23681-2199

ABSTRACT

Thermal inspections of a structure typically utilize a flash or quartz lamp heat source located on the same side of an infrared camera. The heat source provides light energy for heating while the infrared camera measures the surface transient temperature response. The inspection can be difficult for low emissivity surfaces for several reasons. First, the high intensity light can reflect off the surface and cause "burn-in" to the camera's detector. The "burn-in" can take time for the sensors to recover and potentially damage the detector. Secondly, the heat source after pulsing has a transient cool down component. The cool down component can be reflected and therefore superimposed over the structure's thermal response, which can cause an error (false defect indications) in the inspection. Lastly, the heat source is spectrally broad and therefore while heating, infrared components of the heat source can produce non-uniformity in the measured temperature field. Typically for the inspection of low emissivity surfaces, paint or other emissivity enhancing coatings are applied before inspection. In this paper, a pulsed light emitting diodes (PLED) heat source is used. The PLED heat source is spectrally narrow, contained within the visible band, and therefore not detectable by the infrared camera. The PLED heat source is configured to reduce any transient cool down components that could produce false defect indications. The PLED thermal inspections are compared to flash thermography inspections on unpainted aluminum samples with simulated corrosion and an additively manufactured Ti-6AL-4V metal specimens.

Keywords: thermal nondestructive evaluation, low emissivity surfaces, light emitting diode array, aluminum corrosion inspection, porosity detection, additive manufacturing

1. INTRODUCTION

Thermal nondestructive evaluation (NDE) is commonly used for many inspection applications. The most common thermal inspection technique is flash thermography. A high intensity flash lamp (broad spectrum heat source) is used to produce heat that is absorbed by the surface of the structure. An infrared camera is used to record the transient cool down at the surface. Differences in how the sample cools down are used to detect defects, which can change the heat flow. This technique can be applied for the inspection of metals for corrosion, cracks, and disbonded layers, however it can be difficult to apply this inspection on surfaces with low emissivity such as aluminum. Equation 1 describes the relationship for light (independent of wavelength and temperature) incident on a surface. The energy is conserved and therefore the energy reflected (r), absorbed (a), and transmitted (T) must sum up to equal 1.

$$r + a + T = 1 \tag{1}$$

If the transmission (T) is zero, the absorption and the reflectance will sum up to equal 1. For Kirchhoff's law, emittance and absorptance are equal therefore, a good emitter is a good absorber of energy. A high emittance or emissivity value allows for absorption of light energy to be converted to heat and allows the infrared camera to capture the emitted infrared light to measure temperature. Based on Equation 1, with transmittance equal to zero, a low emissivity surface or highly reflective surface can be more difficult to inspect. Generally, more light is required to heat the surface and other background light sources can interfere with the inspection imagery. Current thermal NDE state of the art requires the reflective surface to be covered with a high emissivity layer (either painted or stick on layer) before inspection.

*joseph.n.zalameda@nasa.gov; phone 1 757-864-4793; fax 1 757-864-4914; http://nde.larc.nasa.gov

Another issue is the interaction of the flash lamp cool down or "after glow" after firing. This transient response is superimposed by reflection onto the structure's transient response and therefore can cause false defect indications. The flash lamp heat source is a spectrally broad source that produces light from the ultraviolet through the visible and into the infrared band. The visible band of light is typically passed through glass filters and the ultraviolet and infrared bands are blocked. The blocked energy is absorbed by the filter and causes the filter to heat up and this transient thermal signal can be reflected from the low emissivity reflective surface and measured by the infrared camera.

Even for painted surfaces there still can be a reflected component in the infrared and therefore any influences from the flash lamp heat source cooling down after firing can be detected by the infrared camera. This could also cause a false defect reading. This work describes the use of a high-powered pulsed light emitting diodes (PLED) heat source with optical filters which produces a spectrally narrow band of light for heating and removes thermal transients not related to the inspection and therefore produces an accurate measurement of the surface temperature for inspection. A drawback of the PLED heat source is long pulses are required (typically 1 second or greater) to achieve sufficient heating for inspection, and therefore PLED sources are commonly used as cyclic frequency modulated heat sources. This would require longer inspection times as compared to flash thermography. Previous work by Pickering describes the use of fan cooled light emitting diodes (LED) for long pulse lock-in thermography. Pickering's research showed the promise of the use of light emitting diodes; however, his cooling method was not efficient and therefore became detectable during operation [1]. Additionally, Chulkov and Vavilov studied the use of LED as a frequency modulated heat source applied to a steel sample with good results for corrosion detection [2]. In Chulkov and Vavilov, an emissivity enhancing adhesive layer for detection of hidden corrosion was applied [2]. In this paper, a pulsed light emitting diodes (PLED) heat source is used. The PLED heat source is contained within the visible band and not detectable by the infrared camera. The PLED heat source is configured to reduce false defect indications. The PLED thermal inspections are compared to flash thermography on unpainted aluminum samples with simulated corrosion and on an additively manufactured Ti-6AL-4V metal specimen.

2. PLED INSPECTION SYSTEM

2.1 Configuration of the LED Array and Spectral Light Output

The LED light is shown in Figure 1 and contains 14 high powered XHP70 chips manufactured by CREE.[1] The chips are rated at 12 volts with a maximum current of 2.4 amps. The chips are connected in parallel with two separate circuits. Each circuit is connected to a separate 240 watt regulated power supply. The lamp is computer controlled using solid state relays. The LED array is mounted onto an aluminum heat sink plate which is placed within a flash lamp reflector. The flash lamp reflector is also covered with a clear acrylic plate (1.27 cm thick) to minimize the transmission of infrared light that is produced from the heat generated by the led chips. The PLED spectral light output, shown in Figure 1, was measured using a spectrometer with a spectral range of 340 - 1020 nanometers. The spectrometer spectral range covers bands within the ultraviolet, visible and near infrared. The PLED spectral output, as shown in Figure 1, is contained within the visible band. The acrylic glass will transmit the visible with little loss of light and therefore the acrylic filter will stay cool.

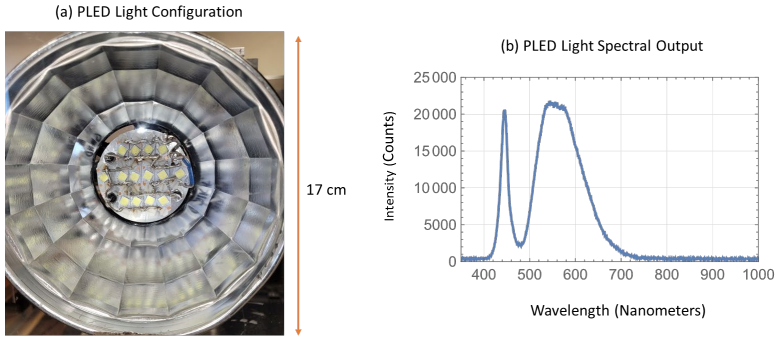

Figure 1: Picture of PLED light configuration with spectral output.

[1] This is not an endorsement by the National Aeronautics and Space Administration (NASA).

2.2 PLED Thermal Inspection System Layout with Direct View Measurement

The thermal inspection layout is shown in Figure 2. The PLED inspection system is comprised of the LED light array located on the same side as the infrared camera. The basic system consists of an IR camera operating in the 3–5 micrometer IR band and a computer for image data acquisition and heat source control. The IR camera was configured with a 13, 25, or 50 mm germanium optical lenses depending on sample size. The focal plane array size of the camera was 640x512 and the camera operated at an 80 Hz frame rate. The camera frame rate was externally triggered and synchronized with the heat source. As previously noted, the PLED heat source is covered with an acrylic filter to block the residual heat of the LED chips and associated wiring. In addition, as shown in Figure 2 there is an acrylic filter placed in front of the infrared camera. The acrylic filter has a viewing hole for the camera lens. Since low emissivity surfaces are being inspected, heat from the infrared camera can be seen in the acquired images if there is no filter. To demonstrate the heat source as "cold heat" or invisible to the infrared camera, the infrared camera was setup pointing directly at the heat source. The setup is shown in Figure 3 wherein the camera is placed approximately 34 cm from the heat source. The heat source is turned on for 5 seconds as shown in Figure 3a. Shown in Figure 3b is the camera output plotted for a single pixel out to 6 seconds or 1 second past the lamp turning off. The single pixel plot has a background intensity subtracted before the lamp is turned on. As shown in Figure 3b there is no obvious detectable heating while the camera is pointed directly at the active heat source. This is due to two main reasons: first the narrow band light is not detectable by the infrared camera and secondly, the narrow band light that is passed through the filter has minimal losses and therefore the filter does not heat up.

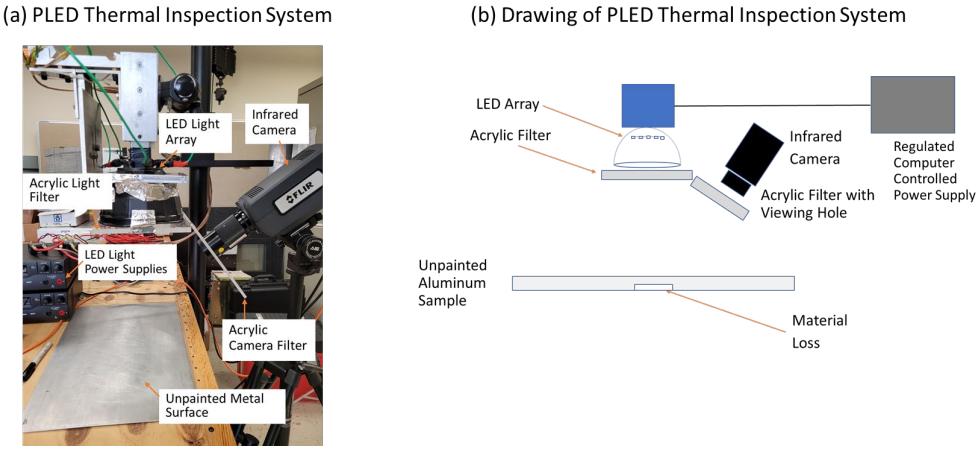

Figure 2: Picture of thermal inspection system using the PLED light.

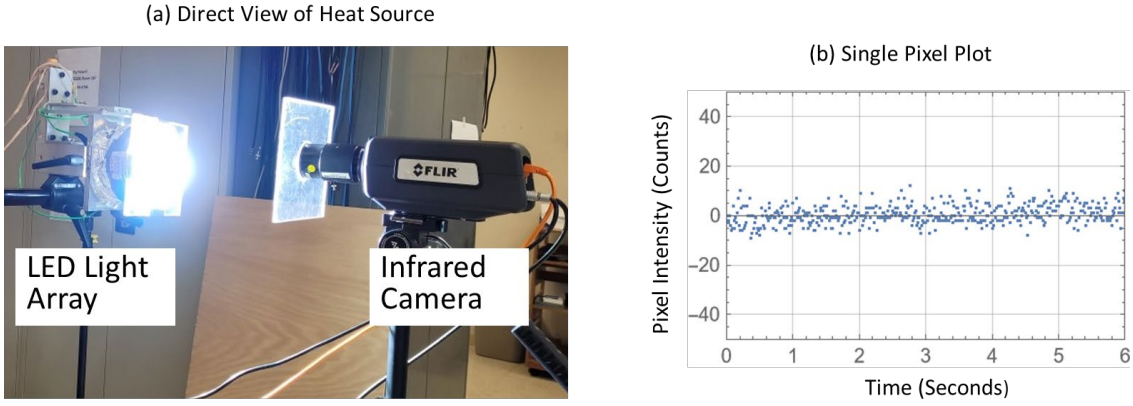

Figure 3: Direct view setup with single pixel camera output plot.

3. SAMPLES INSPECTED AND MEASUREMENT RESULTS

The emissivity of the samples was measured using a technique of comparing the measured surface emissivity to a known value. The technique used a piece of black opaque electrical tape that is applied to the surface of the sample to be measured [3]. The electrical tape emissivity is high at approximately 0.95 [3]. The surface temperature is elevated, and the emissivity is adjusted until the adjacent temperature (measured using a calibrated mid-wave infrared camera) located next to the tape is equal to the measured temperature over the tape with a known emissivity. This measurement is repeated five times to calculate an average emissivity which is shown in Table 1. The aluminum sample, with material loss, is highly oxidized and therefore has an emissivity of 0.35. The unpainted aluminum sample, with circular material loss areas, has a lower emissivity value of 0.21 which indicates the sample is more reflective. A painted aluminum sample is measured for a comparison and that value was 0.90. The polished Ti-6Al-4V disk was built using a laser powder bed fusion additive manufacturing (AM) technique [4]. The disk's emissivity value is 0.39 and is higher as compared to the aluminum samples, however these samples are low compared to a painted aluminum sample emissivity value of 0.90.

Table 1: Comparison of Measured Surface Emissivity

Sample	Average Surface Temperature (Celsius)	Measured Emissivity
Unpainted Aluminum Sample with Material Loss	39.3	0.35 +/- 0.020
Unpainted Aluminum Sample with Circular Material Loss	44.3	0.21 +/- 0.012
Polished Additive Manufactured Ti-6Al-4V Disk	65.8	0.39 +/- 0.017
Painted Aluminum Sample	34.3	0.90 +/- 0.008

3.1 Unpainted Aluminum Plate with Material Loss

An unpainted aluminum plate with backside material loss was inspected using the PLED thermal system. The inspection results were compared to a flash thermography system. The unpainted aluminum plate thickness was approximately 1.63 mm thick. The material loss varied from 0.04 to 1.39 mm which represents material loss of 2.5 to 85 % respectively. The front and back picture of the sample is shown in Figure 4. The material loss areas form the word NASA. Also shown in Figure 5 are the comparison of the PLED inspection to a flash thermography system. The flash data was acquired with a 640 x 512 mid infrared camera, with a 120 Hz frame rate, and 25mm germanium optic. Before processing a background image (acquired before flash) was subtracted. The PLED thermal data was acquired with a 640 x 512 mid infrared camera, with a 100 Hz frame rate, and 25mm germanium optic. A background image (acquired before PLED turn on) was subtracted for the frames processed.

Principal component analysis (PCA) was performed on both the PLED and flash data [5]. This algorithm is based on decomposition of the thermal data into its principal components or eigenvectors. The PCA inspection image is calculated by dot product multiplication of the selected eigenvector times the temperature responses, pixel by pixel. The thermal inspection results were calculated using the 2nd eigenvector which allowed for optimal defect contrast. The PCA time window processing for the flash data was from using images from 0.025 to 0.50 seconds. The PLED output image was obtained by PCA time window processing using images from 0.12 to 2.78 seconds. A longer time window was required, for the PLED inspection, to capture the 1 second step heat pulse and subsequent cool down. As shown in Figure 5, the flash thermal inspection can detect the material loss areas, however two dark bands corresponding to the linear flash tubes are also detected. These flash tubes are placed behind two rectangular glass filters. Because the flash heat source is spectrally broad band, the visible light is transmitted, and the rest of the energy is absorbed. The glass filters therefore heat up thus producing a thermal transient that is superimposed over the sample's thermal response. The PLED thermal inspection image can detect the material loss areas with no heat source reflections.

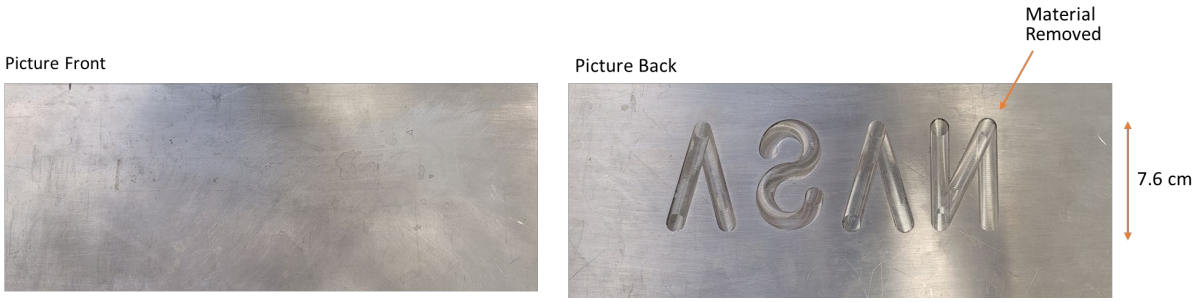

Figure 4: Picture of aluminum plate with material loss.

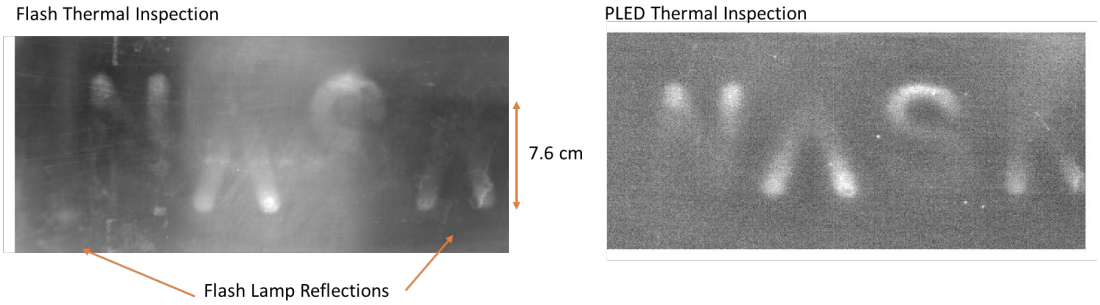

Figure 5: Comparison of inspection results for aluminum plate with material loss using the flash thermal inspection and PLED inspection.

3.2 Unpainted Aluminum Plate with Circular Material Loss Areas

An unpainted aluminum plate with circular material loss defects was inspected using the PLED thermal system. The inspection results were again compared to a flash thermography inspection. The unpainted aluminum plate thickness was approximately 2.1 mm thick. The residual thicknesses of the holes at the hole edges were approximately 0.38 mm for the 19.1 mm diameter holes (A and B) and 0.76 mm for the 12.7 mm diameter holes (C and D). It is important to note the circular hole defects are not flat bottom and therefore increases toward the center to a value of 0.46 mm and 1.0 mm for the 19.1 mm and 12.7 mm holes respectively. The front and back picture of the sample is shown in Figure 6. Shown in Figure 7 are the comparison of the PLED inspection to a flash thermography inspection. PCA was performed on the PLED and flash data sets. The PCA time window processing for the flash data was from using images from 0.1 to 0.83 seconds. The PLED inspection image was obtained by PCA time window processing using images from 0.0625 to 6.25 seconds. A longer time window was required, for the PLED inspection, to capture the 3 second step heat pulse and subsequent cool down. As shown in Figure 7, the flash thermal inspection can detect all four of the material loss areas, however dark vertical bands corresponding to the flash lamp inspection are also detected. The PLED thermal inspection image is able to detect the material loss areas with minimal heat source reflections.

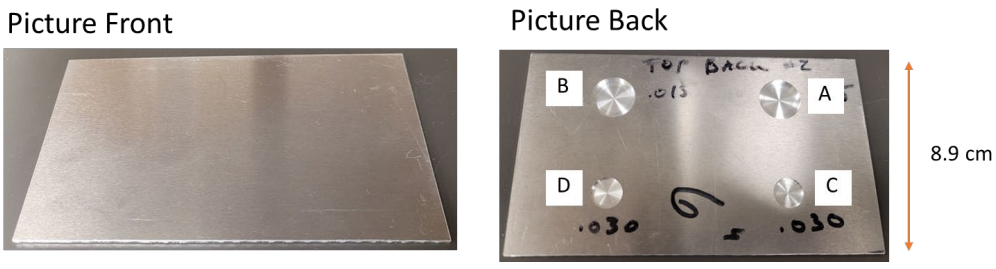

Figure 6: Picture of aluminum plate with material loss.

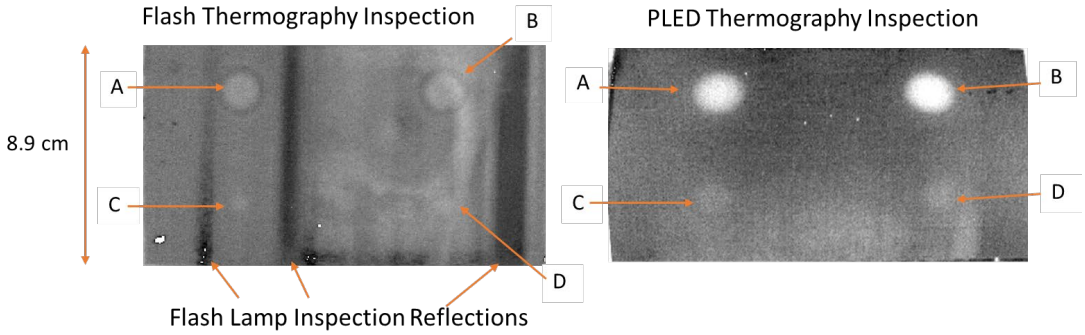

Figure 7: Comparison of inspection results for aluminum plate with circular material loss using the flash and PLED inspection.

3.3 Additive Manufactured Ti-6-4 Polished Disk with Varying Processing Parameters

A disk sample, shown in Figure 8, was fabricated with a laser powder bed fusion AM technique using Ti-6Al-4V powder. The AM technique included a variety of processing parameters combined with specific angular zones to create a wide range of localized process conditions [4]. The angular zones were built with varied laser powers and velocity combinations. Low laser powers with fast scanning velocities resulted in low surface energy densities yielding lack of fusion porosity [4, 6]. A balanced combination of print parameters, power, velocity, and hatch spacing, are expected to result in fully consolidated areas. Angular zones 1-3 in the disk were printed with low surface energy densities which results in lack of fusion porosity.

Zone (n)	Power (watts)	Velocity (mm/sed)	Shape / angular zone [radians]
1	221	1176	Pi/8
2	221	1092	Pi/8
3	221	1008	Pi/8
4	221	924	Pi/8
5	221	840	Pi/8
6	221	756	Pi/8
7	221	672	Pi/8
8	221	588	Pi/8
9	308	1175	Pi/8
10	308	1092	Pi/8
11	308	1008	Pi/8
12	308	924	Pi/8
13	308	840	Pi/8
14	308	756	Pi/8
15	308	672	Pi/8
16	308	588	Pi/8

Figure 8: Picture of polished disk sample with sixteen processing parameter equiangular zones.

The flash and PLED thermal data were acquired with the same system described previously except for a 50 mm germanium optic was used. The PCA time window processing was from 0.167 to 0.833 seconds for the flash data. The PLED output image was obtained by PCA time window processing using images from 0.50 to 5.0 seconds. The PLED heat pulse width was set to 1 second. As shown in Figure 9, the flash thermal inspection can detect the porosity areas, however there are light and dark bands, corresponding to the flash inspection, are also evident. The PLED thermal inspection image can detect the lack of fusion porosity areas, shown as darker areas, with no heat source reflections as shown in Figure 9. The PLED inspection enables greater detail to be resolved.

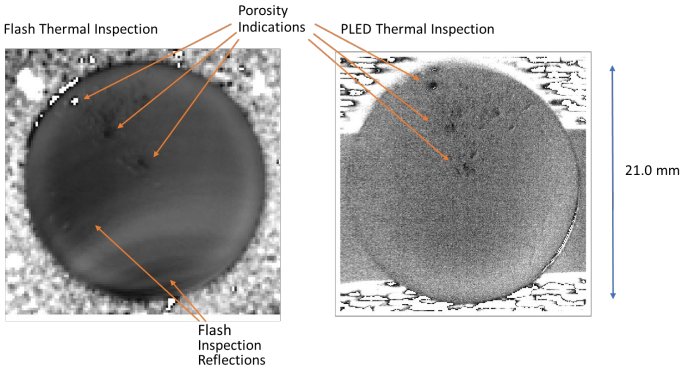

Figure 9: Flash and PLED thermal inspection of polished disk sample.

3.4 Comparison to X-ray CT

X-ray CT measurements, on the polished Ti-6Al-4V disk, were analyzed to investigate near surface porosity for comparison to the thermal inspection indications shown in Figure 9. The small areas a, b, and c thermal inspection indications, shown in Figure 10, compare well to the X-ray CT image. The X-ray CT image is processed by fitting a plane to the top surface and computing the distance to the plane for each segmented voxel corresponding to a void defect. The grey scale is then related to the void depth as shown in Figure 10 legend. The voxel resolution of the X-ray CT was approximately 0.0127 mm for a given X, Y, Z direction. Based on these results, the thermal inspection image appears to be able to detect lack of fusion porosity from 0.125 to 0.250 mm in depth.

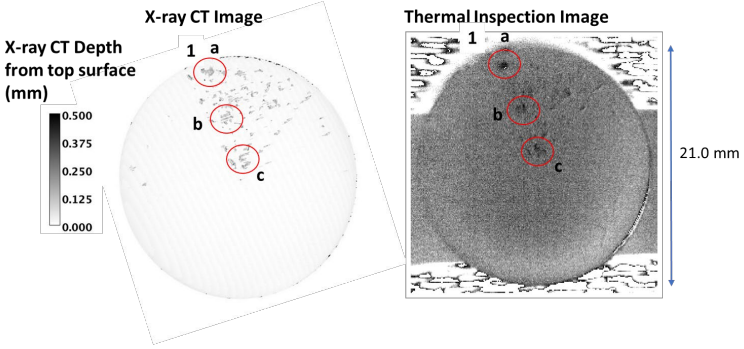

Figure 10: Comparison of disk X-ray CT to thermal inspection image.

4. QUANTITATIVE MEASUREMENT USING THE PLED HEAT SOURCE

4.1 Single Side Inspection Measurement for Thermal Diffusivity on Ti-6-4 Polished Disk

Single side thermography is based on the infrared camera being positioned on the same side of the heat source as shown in the setup in Figure 2. This technique can be quantitative wherein thermal diffusivity is measured for a known thickness [7]. An issue can be the single side thermal measurement can contain errors if any reflections are superimposed onto the samples' thermal response and this can lead to curve fitting errors where the model does not accurately represent the expected thermal response. The PLED heat source can then be advantageous for model-based quantitative single side thermal inspections. A one-dimensional thermal model with constant flux step input at $x = l$, is given in Equation 2, with no flow of heat over $x = 0$, where l is the thickness, t is time, F_0 is the input heat flux, K is the thermal conductivity, and

α is the thermal diffusivity [8]. Equation 2 is then modified to Equation 3 to allow for pulse heating where t_0 is input heat flux time duration produced by the PLED light.

$$T(t,l) = \frac{(F_0\, t\, \alpha)}{K\, l} + \frac{F_0\, l}{K}\left(\frac{1}{3} - \frac{2}{\pi^2}\left(\sum_{n=1}^{nmax} \frac{-1^{2n}}{n^2}\, e^{\frac{-\alpha\, n^2\pi^2\, t}{l^2}}\right)\right) \tag{2}$$

$$T(t,l) = \frac{(F_0\, t\, \alpha)}{K\, l} + \frac{F_0\, l}{K}\left(\frac{1}{3} - \frac{2}{\pi^2}\left(\sum_{n=1}^{nmax} \frac{-1^{2n}}{n^2}\, e^{\frac{-\alpha\, n^2\pi^2\, t}{l^2}}\right)\right) - \frac{(F_0\,(t-t_0)\,\alpha)}{K\, l} - \frac{F_0\, l}{K}\left(\frac{1}{3} - \frac{2}{\pi^2}\left(\sum_{n=1}^{nmax} \frac{-1^{2n}}{n^2}\, e^{\frac{-\alpha\, n^2\pi^2 (t-t_0)}{l^2}}\right)\right) U(t-t_0) \tag{3}$$

The temperature versus time curves were averaged in a 10 x 10 square pixel area located in the center of the polished Ti-6AL-4V disk. An example curve fit [9] using Equation 3 is shown in Figure 11. The heat pulse duration was set to 3 seconds however there was a power supply lag that resulted in a heat pulse width of 2.87 seconds. This was accounted for in the model before curve fitting. The *nmax* was set to 30, $q = F_0/K$, thickness l = 0.307 mm, and the curve fit was a two-parameter fit for variables q and α. The thermal data used in the fit extended out to 6 seconds and the thermal diffusivity value obtained from the fit α = 0.022 cm^2/sec (standard error = +/- 0.0004) with q = 55.0 K/cm (standard error = +/- 0.7759). The literature thermal diffusivity value for solid Ti-6AL-4V (Grade 5) at room temperature is 0.029 cm^2/sec [10]. The curve fit value is less than the literature value and less than previous thermal diffusivity measurements performed using a through transmission technique [11]. This could be due to the input heat flux not being truly a square pulse or the area selected may have had some deeper underlying defects. Despite these possible issues, there is good agreement between the data and the model (Equation 3).

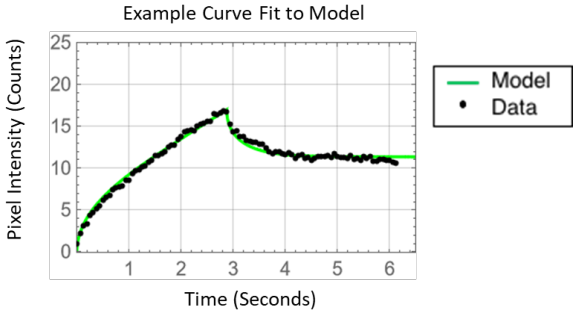

Figure 11: Example curve fit of model to data for a 2.87 second heat pulse.

5. CONCLUSIONS

The PLED heat source has been demonstrated as a viable heat source for thermal inspection of low emissivity surfaces. The PLED heat source advantages are the light is not observable with the mid-wave infrared camera, the light is spectrally narrow and therefore minimal heating was observed as the light would transmit through the infrared filters, and potentially this type of heat source could have cost advantages (potentially 1/2 of the cost or better) as compared to high powered flash heat sources. The model fit revealed good agreement with the thermal data, however, the measured thermal diffusivity using the model was lower than the literature value. More work will be required to measure the actual PLED input heat flux profile to correct for deviations from a true step heating (top hat) temporal profile. Lastly it would be desirable to deliver the heat in a shorter time similar to flash heating. This would allow for the application of the many algorithms developed to process flash data. Lastly, if the PLED heat source can deliver significant heat energy in a shorter time, this potentially would provide shorter inspection times as compared to the PLED heat source being used as a frequency modulated heat source.

ACKNOWLEDGEMENTS

The authors would like to thank William P. Sommers of the Nondestructive Evaluation Sciences Branch for the X-ray CT measurements, James B. Bly for the heat source fabrication, and William B. Bretton for sample fabrication. Also, the authors would like to thank the Transformational Tools and Technologies Project of the NASA Transformative Aeronautics Concepts Program for support of this work.

REFERENCES

[1] Pickering, SG, Chatterjee, K, Almond, DP & Tuli, S 2013, 'LED optical excitation for the long pulse and lock-in thermographic techniques', NDT and E International, vol. 58, pp. 72-77. https://doi.org/10.1016/j.ndteint.2013.04.009.

[2] Chulkov, A.O., Vavilov, V.P. & Malakhov, A.S. A LED-based thermal detector of hidden corrosion flaws. Russ J Nondestructive Test 52, 588–593 (2016). https://doi.org/10.1134/S1061830916100041 Link, R., Ivankov, A., & Riess, N. (2018). Technological Status of Led Techniques - Application in Non-Destructive Testing with Special Emphasis on Magnetic Particle, Penetrant, Visual and Thermographic Inspection. 14th International Conference of the Slovenian Society for Non-Destructive Testing, Sep 4-6, 2017, Bernardin, Slovenia. https://www.ndt.net/?id=22561.

[3] Teledyne FLIR, Use of Low-Cost Materials to Increase Target Emissivity, Use Low-Cost Materials to Increase Target Emissivity | Teledyne FLIR, accessed Feb. 17, 2024.

[4] Hocker, S.J.A., Richter, B., Spaeth, P.W., Kitahara, A.R., Zalameda, J.N., Glaessgen, E.H., 2023. A Point Field Driven Approach to Process Metrics Based on Laser Powder Bed Fusion Additive Manufacturing Models and In-Situ Process Monitoring. JMR. https://doi.org/10.1557/s43578-023-00953-7.

[5] Rajic, N., "Principal Component Thermography for Flaw Contrast Enhancement and Flaw Depth Characterisation in Composite Structures", Composite Structures, Vol. 58, pp. 521--528, (2002).

[6] Tang, M., Pistorius, P.C., Beuth, J.L., 2017. Prediction of lack-of-fusion porosity for powder bed fusion. Additive Manufacturing 14, 39–48. https://doi.org/10.1016/j.addma.2016.12.001.

[7] Winfree W. P. and Heath D. M., "Thermal diffusivity imaging of aerospace materials and structures," Proceedings of SPIE, Thermosense, XXIII 3361, pp. 282–290 (1998).

[8] Carslaw, H. S. and Jaeger J. C., Conduction of Heat in Solids, second edition, DOI : https://doi.org/10.1007/978-3-319-48090-9_9.

[9] WolframResearch(2008), NonlinearModelFit, WolframLanguagefunction, https://reference.wolfram.com/language/ref/NonlinearModelFit.html.

[10] ASM Aerospace Specification Metals Inc., Titanium Ti-6Al-4V (Grade 5), Annealed, ASM Material Data Sheet (matweb.com), Accessed March 29, 2023.

[11] Zalameda, J. N., Hocker, S. A., Frankforter, E. L., Spaeth, P. W., Kitahara, A. R., "Flash thermal diffusivity measurements and inspection of additively manufactured Ti-6Al-4V specimens with varying process parameters," Proc. SPIE 12536, Thermosense: Thermal Infrared Applications XLV, 1253608 (12 June 2023); https://doi.org/10.1117/12.2663546.